# Analysis and Design of a Passive Lossless Snubber in the Two-Inductor Boost Converter with a Variable Input Voltage

Quan Li
Faculty of Engineering and Physical Systems
Central Queensland University
Rockhampton, Queensland, Australia
q.li@cqu.edu.au

Peter Wolfs
Faculty of Engineering and Physical Systems
Central Queensland University
Rockhampton, Queensland, Australia
p.wolfs@cqu.edu.au

## ABSTRACT

*This paper offers a detailed analysis of the non-dissipative snubbers for the hard-switched two-inductor boost converter fed from a sinusoidally modulated two-phase synchronous buck converter. The state analyses and the theoretical waveforms are provided for the three active operation modes of the snubber circuit. The set of border conditions in terms of the buck stage duty ratio for each operation mode is explicitly established. The experimental waveforms are also provided to validate the theoretical analysis.*

## 1. INTRODUCTION

The two-inductor boost converter is an attractive candidate in the application where a high voltage gain is required [1]. However, the resonance between the transformer leakage inductance and the MOSFET output capacitance at the MOSFET turn-off causes the voltage overshoot across the MOSFETs. In order to reduce the MOSFET voltage stress and utilize MOSFETs with low voltage ratings, voltage clamping or snubber circuits must be used. One non-dissipative snubber circuit has been previously proposed for the two-inductor boost converter as shown in Figure 1 [1].

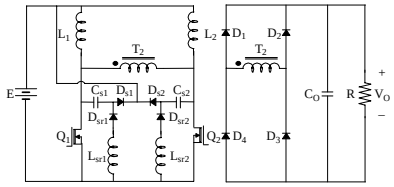

Figure 1: Non-Dissipative Snubbers Proposed in [1]

The current fed two-inductor boost converter employs a variation of the snubber circuit shown in Figure 1 [2]. This paper makes a thorough investigation of the proposed snubber circuit. Four operation modes of the snubber circuit are identified and the ranges of the buck stage duty ratios for the individual operation modes are explicitly established. Detailed state analyses of the snubber circuit for the three active modes are provided. The experimental results of one design example are given at the end of the paper to verify the theoretical analysis.

## 2. NON-DISSIPATIVE SNUBBERS

The non-dissipative snubbers are the desirable solutions in reducing the voltage or current stress in the switching devices as they are able to recover the switching energy to the converter input or output and do not require additional control circuit [3], [4]. The converter shown in Figure 1 employs two sets of snubber circuits, each including one inductor, one capacitor and two diodes. The snubber diode $D_{sr1}$ or $D_{sr2}$ is only forward biased between the instant when the MOSFET $Q_1$ or $Q_2$ turns on and the instant when the current in the snubber inductor $L_{sr1}$ or $L_{sr2}$ reaches zero. If the current in the snubber inductor on one side reaches zero before the MOSFET on the other side turns on, the snubber inductor can be shared by the snubber circuits for both MOSFETs and only one snubber inductor is required. Figure 2 shows the current fed two-inductor boost converter with the non-dissipative snubbers using only one snubber inductor [2]. Space-saving is possible as the inductors are generally the biggest in size among the components used in the snubber circuit.

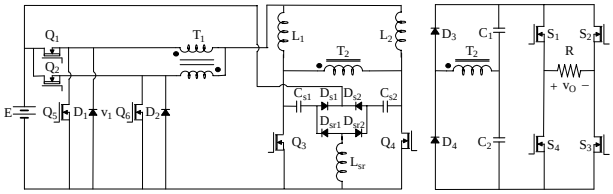

Figure 2: Current fed two-inductor boost converter

## 3. STATE ANALYSES

The two-inductor boost cell in Figure 2 is fed from a sinusoidally modulated two-phase synchronous buck converter and the average input voltage and current follow the rectified sinusoidal waveforms. Therefore, variable peak MOSFET voltages exist in the converter without the snubber. The snubber circuit is only required to be active when the buck stage duty ratio is relatively high. This avoids the energy circulation and the conduction power loss due to the parasitic components in the snubber circuit under low buck stage duty ratios, under which the peak MOSFET voltages are naturally within the desired voltage level. The snubber circuit is analyzed using the equivalent circuit in Figure 3.

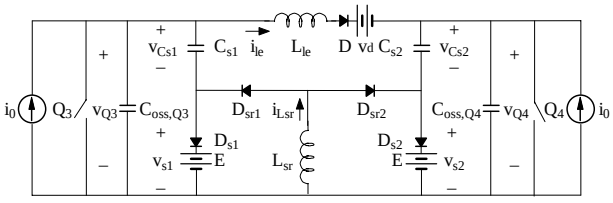

Figure 3: Equivalent snubber circuit

In Figure 3, the current source $i_0$ models the inductor $L_1$ or $L_2$. The MOSFET $Q_3$ or $Q_4$ output capacitance is

$C_{oss,Q3} = C_{oss,Q4} = C_{oss}$. The snubber capacitance is $C_{s1} = C_{s2} = C_s$. The transformer $T_2$ leakage inductance is $L_{le}$. The voltage source $v_d$ is the capacitor $C_1$ or $C_2$ voltage reflected to the transformer $T_2$ primary and the diode D corresponds to the diodes in the voltage-doubler rectifier. The arrangement for $v_d$ and D in Figure 3 assumes a positive current $i_{le}$ as illustrated and their polarities reverse when $i_{le}$ becomes negative. $C_{oss,Q3}$ or $C_{oss,Q4}$ can be neglected whenever $C_{s1}$ or $C_{s2}$ is actively involved in the operation as $C_s >> C_{oss}$. $C_{oss,Q3}$ or $C_{oss,Q4}$ is also neglected when $i_{le}$ first reaches $i_0$ or $-i_0$ and damped oscillations happen between $L_{le}$ and $C_{oss,Q3}$ or $C_{oss,Q4}$ due to the parasitic resistances in the circuit.

It is established that the snubber circuit can operate in four modes under different $v_{Cs0}$, the initial snubber capacitor voltage before the MOSFET turns off. The snubber circuit returns the energy to the voltage source supply E only in Mode 1 and does not in Modes 2 and 3 although it is active. The snubber circuit is not active in Mode 4. The state analyses of the individual operation modes are given first against $v_{Cs0}$ over one switching period starting from $Q_3$ turn-off. The range of the buck stage MOSFET $Q_1$ or $Q_2$ duty ratio $D_{buck}$ for each operation mode will be determined in the due course.

Before $Q_3$ turns off at $t = 0$, $Q_3$ and $Q_4$ are both on. In each operation mode, the snubber capacitor voltage $v_{Cs1}$, the snubber inductor current $i_{Lsr}$, the transformer primary current $i_{le}$, the MOSFET $Q_3$ drain source voltage $v_{Q3}$ and the snubber diode $D_{s1}$ anode voltage $v_{s1}$ will be discussed. It is worth mentioning that before $Q_3$ turns on later in the cycle, $L_{sr}$ is not involved in the operation of the snubber circuit for $Q_3$. Therefore, $i_{Lsr}$ will not be included in the analyses of the states before $Q_3$ turns on. Also when $i_{le}$ finally becomes negative after $Q_4$ turns off, the polarities of $v_d$ and D will be reversed and $L_{le}$, D and $v_d$ will interact with the snubber circuit for $Q_4$. Therefore, $i_{le}$ will not be included in the analyses of the states after $Q_3$ turns on.

### 3.1. MODE 1

In Mode 1, $v_{Cs0} = -E$ and the snubber circuit becomes active at the instant when $Q_3$ turns off. The snubber circuit moves through six states in one switching period, which are shown in Figure 4.

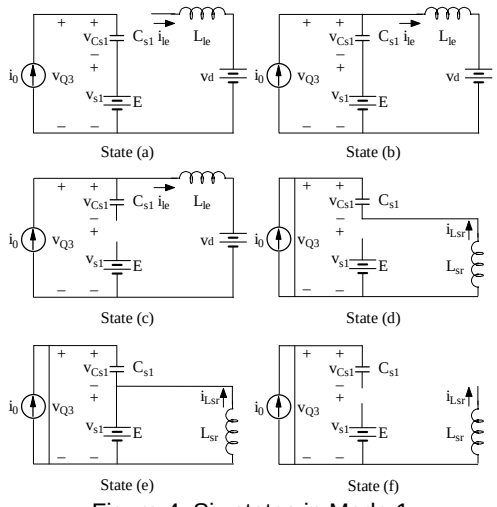

Figure 4: Six states in Mode 1

- State (a) ($0 \le t \le t_1$): This state starts when $Q_3$ turns off at $t = 0$. The diode $D_{s1}$ is forward biased and the current source $i_0$ linearly charges $C_{s1}$. The diodes D and $D_{sr1}$ are both reverse biased. The initial conditions are $v_{Cs1}(0) = -E$ and $i_{le}(0) = 0$. The equations are:

$$v_{Cs1}(t) = -E + (i_0 / C_s)t \quad (1)$$
$$i_{le}(t) = 0 \quad (2)$$
$$v_{Q3}(t) = (i_0 / C_s)t \quad (3)$$
$$v_{s1}(t) = E \quad (4)$$

- State (b) ($t_1 \le t \le t_2$): This state starts when $v_{Q3}$ reaches $v_d$ at $t_1 = v_d C_s / i_0$. Both of the diodes $D_{s1}$ and D are forward biased and $C_{s1}$ resonates with $L_{le}$. The diode $D_{sr1}$ remains reverse biased. The initial conditions are $v_{Cs1}(t_1) = v_d - E$ and $i_{le}(t_1) = 0$. In this state, Equation (4) is valid. The other equations are:

$$v_{Cs1}(t) = v_d - E + i_0 Z_1 \sin\omega_1(t - t_1) \quad (5)$$
$$i_{le}(t) = i_0 - i_0 \cos\omega_1(t - t_1) \quad (6)$$
$$v_{Q3}(t) = v_d + i_0 Z_1 \sin\omega_1(t - t_1) \quad (7)$$

where $Z_1 = \sqrt{L_{le}/C_s}$ is the characteristic impedance and $\omega_1 = 1/\sqrt{L_{le}C_s}$ is the characteristic angular resonant frequency of the resonant tank.

- State (c) ($t_2 \le t \le t_3$): This state starts when $i_{le}$ reaches $i_0$ at $t_2 = t_1 + \pi/(2\omega_1)$. The diode $D_{s1}$ becomes reverse biased. The diode D remains forward biased and the current source $i_0$ flows through $L_{le}$ and $v_d$. The diode $D_{sr1}$ is still reverse biased. The equations are:

$$v_{Cs1}(t) = v_d - E + i_0 Z_1 \quad (8)$$
$$i_{le}(t) = i_0 \quad (9)$$
$$v_{Q3}(t) = v_d \quad (10)$$
$$v_{s1}(t) = E - i_0 Z_1 \quad (11)$$

- State (d) ($t_3 \le t \le t_4$): This state starts when $Q_3$ turns on at $t_3 = (1 - D_{boost})T_{boost}$, where $D_{boost}$ and $T_{boost}$ are respectively the boost stage duty ratio and switching period. The diode $D_{s1}$ remains reverse biased. The diode $D_{sr1}$ becomes forward biased and $L_{sr}$ resonates with $C_{s1}$. The initial conditions are $v_{Cs1}(t_3) = v_d - E + i_0 Z_1$ and $i_{Lsr}(t_3) = 0$. The equations are:

$$v_{Cs1}(t) = (v_d - E + i_0 Z_1)\cos\omega_2(t - t_3) \quad (12)$$
$$i_{Lsr}(t) = [(v_d - E + i_0 Z_1)/Z_2]\sin\omega_2(t - t_3) \quad (13)$$
$$v_{Q3}(t) = 0 \quad (14)$$
$$v_{s1}(t) = (E - v_d - i_0 Z_1)\cos\omega_2(t - t_3) \quad (15)$$

where $Z_2 = \sqrt{L_{sr}/C_s}$ is the characteristic impedance and $\omega_2 = 1/\sqrt{L_{sr}C_s}$ is the characteristic angular resonant frequency of the resonant tank.

- State (e) ($t_4 \le t \le t_5$): This state starts when $v_{Cs1}$ reaches –E at $t_4$. The diode $D_{s1}$ becomes forward biased and the diode $D_{sr1}$ remains forward biased. The voltage

source E linearly discharges $L_{sr}$ and the energy in $L_{sr}$ is returned to E. The initial conditions are $v_{Cs1}(t_4) = -E$ and $i_{Lsr}(t_4) = [(v_d - E + i_0 Z_1)/Z_2]\sin\omega_2(t_4 - t_3)$. In this state, Equations (4) and (14) are valid. The other equations are:

$$v_{Cs1}(t) = -E \quad (16)$$

$$i_{Lsr}(t) = i_{Lsr}(t_4) - (E/L_{sr})(t - t_4) \quad (17)$$

- State (f) ($t_5 \le t \le t_6$): This state starts when $i_{Lsr}$ reaches 0 at $t_5 = t_4 + i_{Lsr}(t_4)L_{sr}/E$. The snubber circuit will become active when $Q_3$ turns off again at $t_6 = T_{boost}$ except that $L_{sr}$ will be earlier involved in the operation of the snubber circuit for $Q_4$ when $Q_4$ turns on.

### 3.2. MODE 2

In Mode 2, $-E < v_{Cs0} < 0$ and the snubber circuit becomes active after $Q_3$ turns off but before $v_{Q3}$ reaches $v_d$. The snubber circuit moves through six states in one switching period, which are shown in Figure 5.

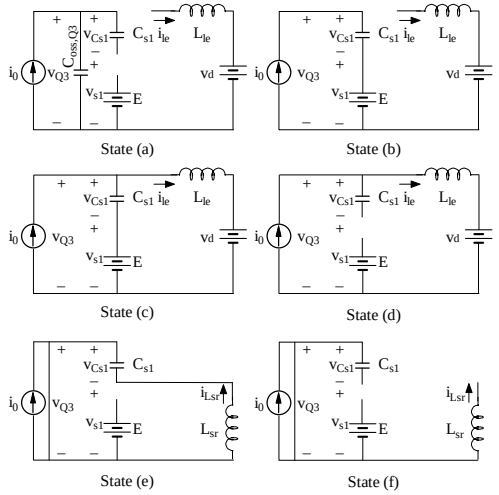


Figure 5: Six states in Mode 2

- State (a) ($0 \le t \le t_1$): This state starts when $Q_3$ turns off at $t = 0$. The diode $D_{s1}$ is reverse biased and the current source $i_0$ linearly charges $C_{oss,Q3}$. The diodes D and $D_{sr1}$ are both reverse biased. The initial conditions are $v_{Q3}(0) = 0$, $v_{Cs1}(0) = v_{Cs0}$ and $i_{le}(0) = 0$. In this state, Equation (2) is valid. The other equations are:

$$v_{Cs1}(t) = v_{Cs0} \quad (18)$$

$$v_{Q3}(t) = (i_0/C_{oss})t \quad (19)$$

$$v_{s1}(t) = -v_{Cs0} + (i_0/C_{oss})t \quad (20)$$

- State (b) ($t_1 \le t \le t_2$): This state starts when $v_{s1}$ reaches E at $t_1 = (E + v_{Cs0})C_{oss}/i_0$ and the snubber circuit operates in the same way as State (a) in Mode 1. The initial conditions are $v_{Cs1}(t_1) = v_{Cs0}$ and $i_{le}(t_1) = 0$. In this state, Equations (2) and (4) are valid. The other equations are:

$$v_{Cs1}(t) = v_{Cs0} + (i_0/C_s)(t - t_1) \quad (21)$$

$$v_{Q3}(t) = E + v_{Cs0} + (i_0/C_s)(t - t_1) \quad (22)$$

- State (c) ($t_2 \le t \le t_3$): This state starts when $v_{Q3}$ reaches $v_d$ at $t_2 = t_1 + (v_d - E - v_{Cs0})C_s/i_0$ and the snubber circuit operates in the same way as State (b) in Mode 1. The initial conditions are $v_{Cs1}(t_2) = v_d - E$ and $i_{le}(t_2) = 0$. In this state, Equation (4) is valid. The other equations are:

$$v_{Cs1}(t) = v_d - E + i_0 Z_1 \sin\omega_1(t - t_2) \quad (23)$$

$$i_{le}(t) = i_0 - i_0 \cos\omega_1(t - t_2) \quad (24)$$

$$v_{Q3}(t) = v_d + i_0 Z_1 \sin\omega_1(t - t_2) \quad (25)$$

- State (d) ($t_3 \le t \le t_4$): This state starts when $i_{le}$ reaches $i_0$ at $t_3 = t_2 + \pi/(2\omega_1)$ and the snubber circuit operates in the same way as State (c) in Mode 1. In this state, Equations (8) to (11) are valid.

- State (e) ($t_4 \le t \le t_5$): This state starts when $Q_3$ turns on at $t_4 = (1 - D_{boost})T_{boost}$ and the snubber circuit operates in the same way as State (d) in Mode 1. The initial conditions are $v_{Cs1}(t_4) = v_d - E + i_0 Z_1$ and $i_{Lsr}(t_4) = 0$. In this state, Equation (14) is valid. The other equations are:

$$v_{Cs1}(t) = (v_d - E + i_0 Z_1)\cos\omega_2(t - t_4) \quad (26)$$

$$i_{Lsr}(t) = [(v_d - E + i_0 Z_1)/Z_2]\sin\omega_2(t - t_4) \quad (27)$$

$$v_{s1}(t) = (E - v_d - i_0 Z_1)\cos\omega_2(t - t_4) \quad (28)$$

- State (f) ($t_5 \le t \le t_6$): This state starts when $i_{Lsr}$ reaches 0 at $t_5 = t_4 + \pi/\omega_2$ and the snubber circuit operates in the same way as State (f) in Mode 1.

### 3.3. MODE 3

In Mode 3, $-E < v_{Cs0} < 0$ but the absolute value of $v_{Cs0}$ is so small that the snubber circuit is active after $v_{Q3}$ reaches $v_d$. The snubber circuit moves through six states in one switching period, which are shown in Figure 6.

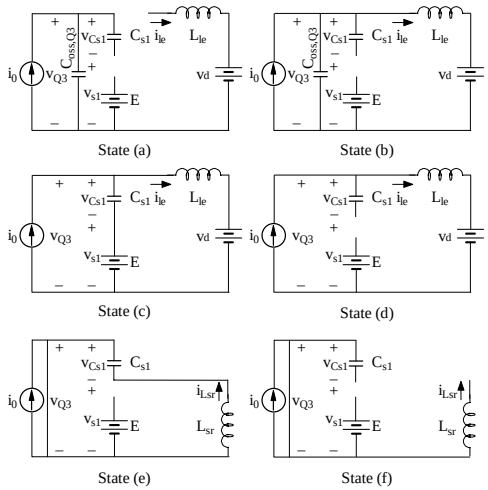


Figure 6: Six states in Mode 3

- State (a) ($0 \le t \le t_1$): This state starts when $Q_3$ turns off at $t = 0$ and the snubber circuit operates in the same way as State (a) in Mode 2. In this state, Equations (2) and (18) to (20) are valid.

- State (b) ($t_1 \le t \le t_2$): This state starts when $v_{Q3}$ reaches $v_d$ at $t_1 = v_d C_{oss} / i_0$. The diode D becomes forward biased and $C_{oss,Q3}$ resonates with $L_{le}$. The diodes $D_{s1}$ and $D_{sr1}$ remain reverse biased. The initial conditions are $v_{Q3}(t_1) = v_d$, $v_{Cs1}(t_1) = v_{Cs0}$ and $i_{le}(t_1) = 0$. In this state, Equation (18) is valid. The other equations are:

$$i_{le}(t) = i_0 - i_0 \cos \omega_3 (t - t_1) \quad (29)$$

$$v_{Q3}(t) = v_d + i_0 Z_3 \sin \omega_3 (t - t_1) \quad (30)$$

$$v_{s1}(t) = v_d - v_{Cs0} + i_0 Z_3 \sin \omega_3 (t - t_1) \quad (31)$$

where $Z_3 = \sqrt{L_{le} / C_{oss}}$ is the characteristic impedance and $\omega_3 = 1/\sqrt{L_{le} C_{oss}}$ is the characteristic angular resonant frequency of the resonant tank.

- State (c) ($t_2 \le t \le t_3$): This state starts when $v_{s1}$ reaches E at $t_2$ and the snubber circuit operates in the same way as State (b) in Mode 1. The initial conditions are $v_{Cs1}(t_2) = v_{Cs0}$ and $i_{le}(t_2) = i_0 - i_0 \cos \omega_3 (t_2 - t_1)$. In this state, Equation (4) is valid. The other equations are:

$$v_{Cs1}(t) = v_d - E + [i_0 - i_{le}(t_2)] Z_1 \sin \omega_1 (t - t_2) - (v_d - E - v_{Cs0}) \cos \omega_1 (t - t_2) \quad (32)$$

$$i_{le}(t) = i_0 - [(v_d - E - v_{Cs0}) / Z_1] \sin \omega_1 (t - t_2) - [i_0 - i_{le}(t_2)] \cos \omega_1 (t - t_2) \quad (33)$$

$$v_{Q3}(t) = v_d + [i_0 - i_{le}(t_2)] Z_1 \sin \omega_1 (t - t_2) - (v_d - E - v_{Cs0}) \cos \omega_1 (t - t_2) \quad (34)$$

- State (d) ($t_3 \le t \le t_4$): This state starts when $i_{le}$ reaches $i_0$ at $t_3$ and the snubber circuit operates in the same way as State (c) in Mode 1. In this state, Equations (9) and (10) are valid. The other equations are:

$$v_{Cs1}(t) = v_{Cs1}(t_3) \quad (35)$$

$$v_{s1}(t) = v_d - v_{Cs1}(t_3) \quad (36)$$

- State (e) ($t_4 \le t \le t_5$): This state starts when $Q_3$ turns on at $t_4 = (1 - D_{boost}) T_{boost}$ and the snubber circuit operates in the same way as State (d) in Mode 1. The initial conditions are $v_{Cs1}(t_4) = v_{Cs1}(t_3)$ and $i_{Lsr}(t_4) = 0$. In this state, Equation (14) is valid. The other equations are:

$$v_{Cs1}(t) = v_{Cs1}(t_3) \cos \omega_2 (t - t_4) \quad (37)$$

$$i_{Lsr}(t) = [v_{Cs1}(t_3) / Z_2] \sin \omega_2 (t - t_4) \quad (38)$$

$$v_{s1}(t) = -v_{Cs1}(t_3) \cos \omega_2 (t - t_4) \quad (39)$$

- State (f) ($t_5 \le t \le t_6$): This state starts when $i_{Lsr}$ reaches 0 at $t_5 = t_4 + \pi / \omega_2$ and the snubber circuit operates in the same way as State (f) in Mode 1.

### 3.4. MODE 4

In Mode 4, $v_{Cs0} = 0$ and the snubber circuit is not active in the converter. The diodes in the snubber circuit remain reverse biased at all times.

## 4. BORDER CONDITIONS

The operation mode of the snubber circuit is intrinsically determined by $D_{buck}$ as $C_{s1}$ is charged to different voltage levels at the end of State (e) in each mode under different values of $D_{buck}$. In order to find the border conditions in terms of $D_{buck}$, the following two converter equations must be used, where $P_{avg}$ is the converter average output power.

$$v_d = D_{buck} E / (1 - D_{boost}) \quad (40)$$

$$i_0 = D_{buck} P_{avg} / E \quad (41)$$

In Mode 1, $v_{Cs1}$ must reach –E before $i_{Lsr}$ reaches 0 in State (d). According to Equations (12) and (13), the border condition is:

$$2E - v_d - i_0 Z_1 = 0 \quad (42)$$

Substituting Equations (40) and (41) to (42) and replacing $D_{buck}$ with $D_{buck,1}$ yield:

$$D_{buck,1} = 2 \Big/ \left( \frac{1}{1 - D_{boost}} + \frac{P_{avg}}{E^2} Z_1 \right) \quad (43)$$

Therefore the range of $D_{buck}$ for the snubber circuit to operate in Mode 1 is $D_{buck} \ge D_{buck,1}$. If $D_{buck} < D_{buck,1}$, the snubber circuit starts to operate in Mode 2. It is also required that $v_{s1}$ reaches E before $v_{Q3}$ reaches $v_d$ in State (a) in this mode. According to Equations (19), (20) and (26), the lower border condition is:

$$2E - 2v_d - i_0 Z_1 = 0 \quad (44)$$

Substituting Equations (40) and (41) to (44) and replacing $D_{buck}$ with $D_{buck,2}$ yield:

$$D_{buck,2} = 1 \Big/ \left( \frac{1}{1 - D_{boost}} + \frac{P_{avg}}{2E^2} Z_1 \right) \quad (45)$$

Therefore the range of $D_{buck}$ for the snubber circuit to operate in Mode 2 is $D_{buck,2} \le D_{buck} < D_{buck,1}$. If $D_{buck} < D_{buck,2}$, the snubber circuit starts to operate in Mode 3. It is also required that $v_{s1}$ reaches E in State (b) in this mode. It can be established that $v_{Cs0} = 0$ when the snubber circuit operates at the border between Modes 3 and 4. According to Equation (31), the lower border condition is:

$$v_d + i_0 Z_3 = E \quad (46)$$

Substituting Equations (40) and (41) to (46) and replacing $D_{buck}$ with $D_{buck,3}$ yield:

$$D_{buck,3} = 1 \Big/ \left( \frac{1}{1 - D_{boost}} + \frac{P_{avg}}{E^2} Z_3 \right) \quad (47)$$

Therefore the range of $D_{buck}$ for the snubber circuit to operate in Mode 3 is $D_{buck,3} < D_{buck} < D_{buck,2}$. If $D_{buck} \le D_{buck,3}$, the snubber circuit starts to operate in Mode 4, where the snubber circuit is not active in the converter operation.

## 5. SNUBBER CIRCUIT DESIGN

As the leakage inductance is determined by the design of the transformer $T_2$, the peak switch voltage over a low frequency cycle decreases with a larger snubber capacitance according to Equation (7) while the range of $D_{buck}$ for Mode 1 increases with a smaller snubber capacitance according to Equation (43). The snubber capacitance is designed as 0.1 μF to obtain a reasonable peak switch voltage and range of $D_{buck}$ for Mode 1. Once the snubber capacitance is determined, the peak snubber inductor current over a low frequency cycle decreases with a larger snubber inductance according to Equation (13) while the duration of the non-zero snubber inductor current decreases with a smaller snubber inductance according to Equations (12), (17), (27) and (38). The snubber inductance is designed as 10 μH and the durations of the non-zero snubber inductor current are short enough to allow the sharing of one snubber inductor by the two snubber circuits for $Q_3$ and $Q_4$.

The border conditions can be finally calculated as $D_{buck,1} = 0.706$, $D_{buck,2} = 0.396$ and $D_{buck,3} = 0.119$ with the following parameters:

- The converter input voltage $E = 20\,V$ and average power $P_{avg} = 100\,W$.
- The two-inductor boost cell switching frequency $f_{boost} = 75\ kHz$ and duty ratio $D_{boost} = 0.55$.
- The transformer $T_2$ leakage inductance $L_{le} = 0.60\ \mu H$ and the MOSFET $Q_3$ Infineon SPB80N06S2L-07 output capacitance $C_{oss} = 990\ pF$.

Figures 7 to 9 respectively shows the theoretical waveforms of the three active operation modes when $D_{buck} = 1$, $D_{buck} = 0.60$ and $D_{buck} = 0.35$. Mode 1 is characterized by the $v_{Q3}$ waveform with a small voltage slope at the turn-off due to the linear charging of the relatively large snubber capacitance. Mode 2 is characterized by the $v_{Q3}$ waveform with an initial large voltage slope followed by a small voltage slope at the turn-off due to the linear charging of the much smaller MOSFET output capacitance first and then the larger snubber capacitance. Mode 3 is characterized by the $v_{Q3}$ waveform with large voltage slopes at the turn-off almost until $v_{Q3}$ reaches its peak due to the linear charging of the MOSFET output capacitance first and the resonance between the MOSFET output capacitance and the transformer leakage inductance. Then the resonance between the snubber capacitance and the transformer leakage inductance only happens in a very short time before the transformer primary current reaches $i_0$.

## 6. EXPERIMENTAL WAVEFORMS

The experimental waveforms of the snubber circuit operating in Modes 1, 2 and 3 are respectively shown in Figures 10 to 12.

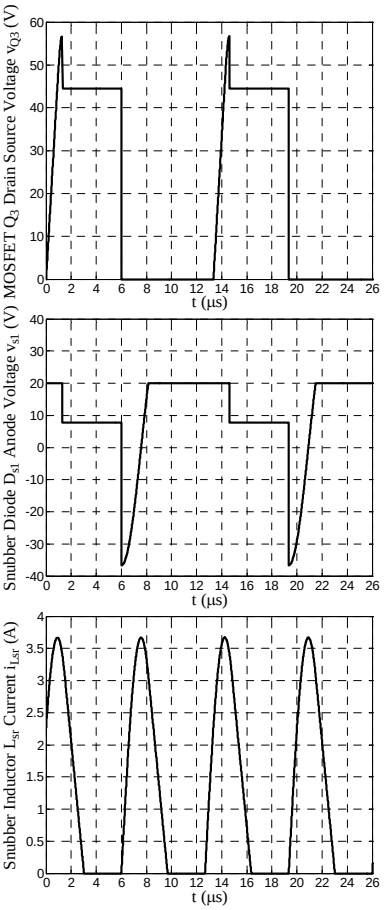


Figure 7: Mode 1 theoretical waveforms

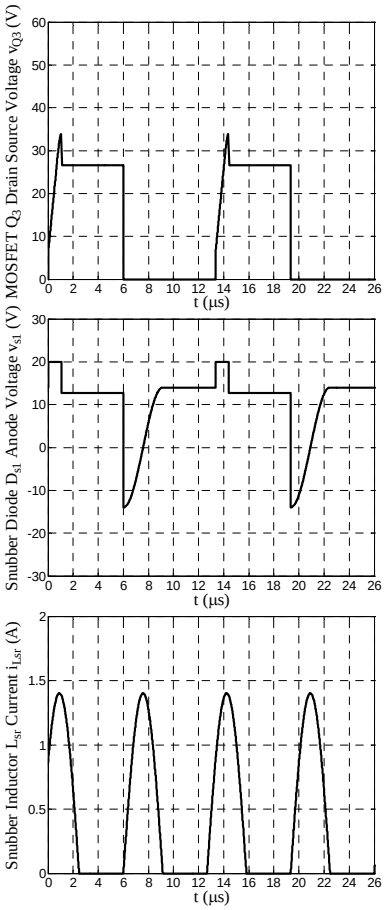


Figure 8: Mode 2 theoretical waveforms

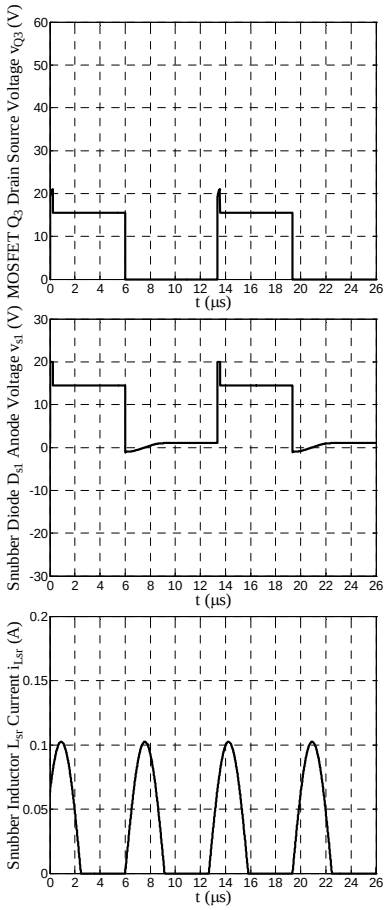


Figure 9: Mode 3 theoretical waveforms

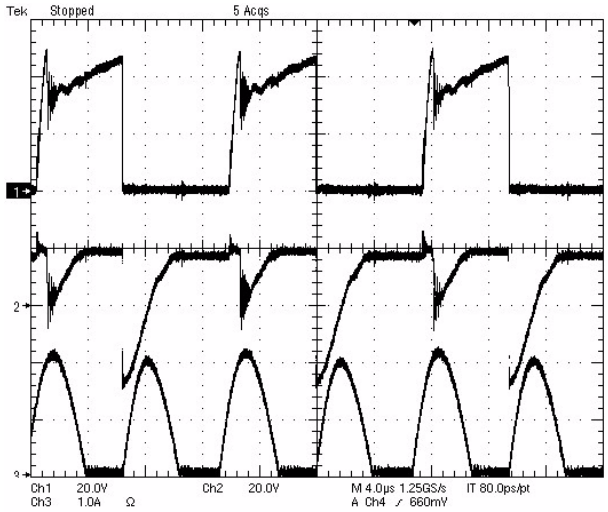


Figure 10: Mode 1 experimental waveforms

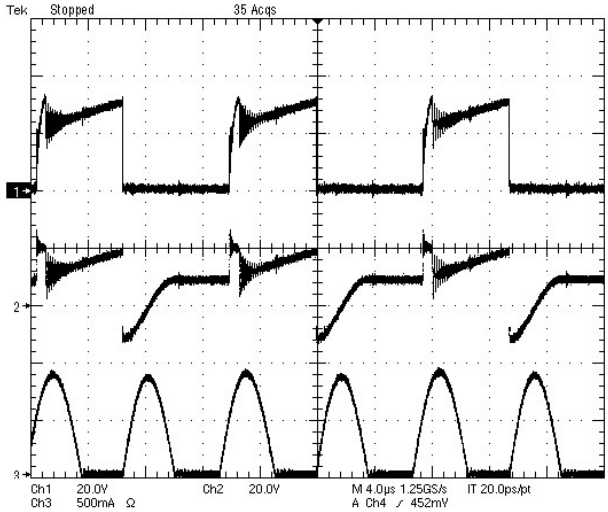


Figure 11: Mode 2 experimental waveforms

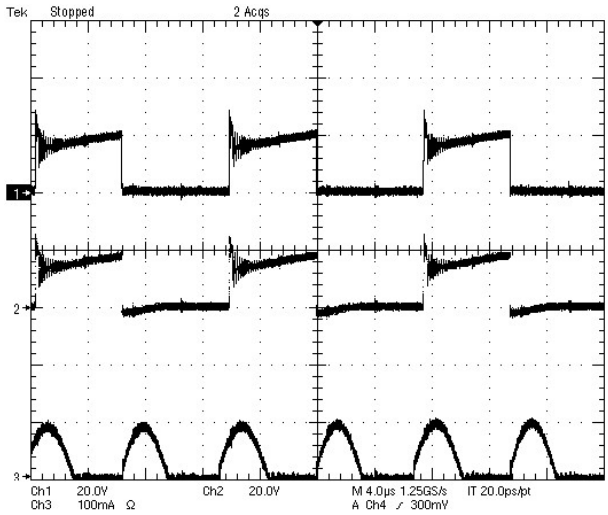


Figure 12: Mode 3 experimental waveforms

The key components used in the snubber circuit are:

- Capacitors $C_{s1}$ and $C_{s2}$ – Kemet class X7R surface mount capacitor, $C = 0.1\ \mu F$ , $V_{dc} = 50\ V$ .
- Inductor $L_{sr}$ – Core type Siemens RM7 with 0.16 mm air gap in the centre pole, ferrite grade Siemens N48, inductor winding $N_L = 7$ turns.
- Diodes $D_{s1}$, $D_{s2}$, $D_{sr1}$ and $D_{sr2}$ – Fairchild SS26, $I_F = 2.0\ A$ , $V_{RRM} = 60\ V$ , $V_F = 0.7\ V$ .

From top to bottom, Figures 10 to 12 respectively shows the waveforms of $v_{Q3}$, $v_{s1}$ and $i_{Lsr}$. The buck stage duty ratios in Figures 10 and 12 are respectively around $D_{buck} = 0.84$ , $D_{buck} = 0.57$ and $D_{buck} = 0.38$ and these are estimated by the individual instantaneous converter output voltages captured by the oscilloscope. The characteristics of the individual operation modes can be clearly observed although the buck duty ratio is not a constant under the consecutive high frequency cycles in the practical converter. Some differences between the theoretical and the experimental waveforms lie on the damped oscillations after $v_{Q3}$ reaches its peak due to the resonance between the MOSFET output capacitance and the transformer leakage inductance and as well on $v_d$ being not a constant due to the charging of the capacitors in the rectification stage of the boost cell. The experimental results show that the peak MOSFET voltage is limited to 55 V. This allows the MOSFETs with low on resistances to be used and enables the 100-W converter to achieve 92% efficiency.

## 7. CONCLUSIONS

This paper analyses in detail the non-dissipative snubbers for the current fed two-inductor boost converter, which has a variable input voltage to the boost cell. The passive snubber circuit has a simple design and is capable of recovering the switching energy at high buck stage duty ratios. It is established that the snubber circuit is able to operate in three active and one inactive modes over one low frequency cycle. The state analyses are elaborated for the three active operation modes and the explicit border conditions for the individual operation modes are found. Both of the theoretical and the experimental waveforms are provided and the characteristics of the individual operation modes match well in the corresponding waveforms.

## REFERENCES

[1] P. J. Wolfs, "A Current-Sourced DC-DC Converter Derived via the Duality Principle from the Half-Bridge Converter," *IEEE Trans. Ind. Electron.*, Vol. 40, No. 1, pp. 139-144, Feb. 1993.

[2] Q. Li and P. Wolfs, "A Current Fed Two-Inductor Boost Converter for Grid Interactive Photovoltaic Applications", in *Proc. AUPEC*, 2004.

[3] K. M. Smith, Jr. and K. M. Smedley, "Properties and Synthesis of Passive Lossless Soft-Switching PWM Converters," *IEEE Trans. Power Electron.*, Vol. 14, No. 5, pp. 890-899, Sept. 1999.

[4] J. D. Van Wyk and J. A. Ferreira, "Transistor Inverter Design Optimization in the Frequency Range above 5 kHz up to 50 kVA," *IEEE Trans. Ind. Applicat.*, Vol. 19, No. 2, pp. 296-302, Mar./Apr. 1983.